Title

VELOCITY PLOTS AND CAPTURE ZONES OF PUMPING CENTERS FOR GROUND WATER INVESTIGATIONS

Authors

Keely, J.F.
Tsang, C.F.

Publication Date

1983-05-01

Lawrence Berkeley Laboratory
UNIVERSITY OF CALIFORNIA

EARTH SCIENCES DIVISION

Presented at the Third National Symposium on Aquifer Restoration and Groundwater Monitoring, Columbus, OH, May 25-27, 1983

VELOCITY PLOTS AND CAPTURE ZONES OF PUMPING CENTERS FOR GROUND WATER INVESTIGATIONS

J.F. Keely and C.F. Tsang

May 1983

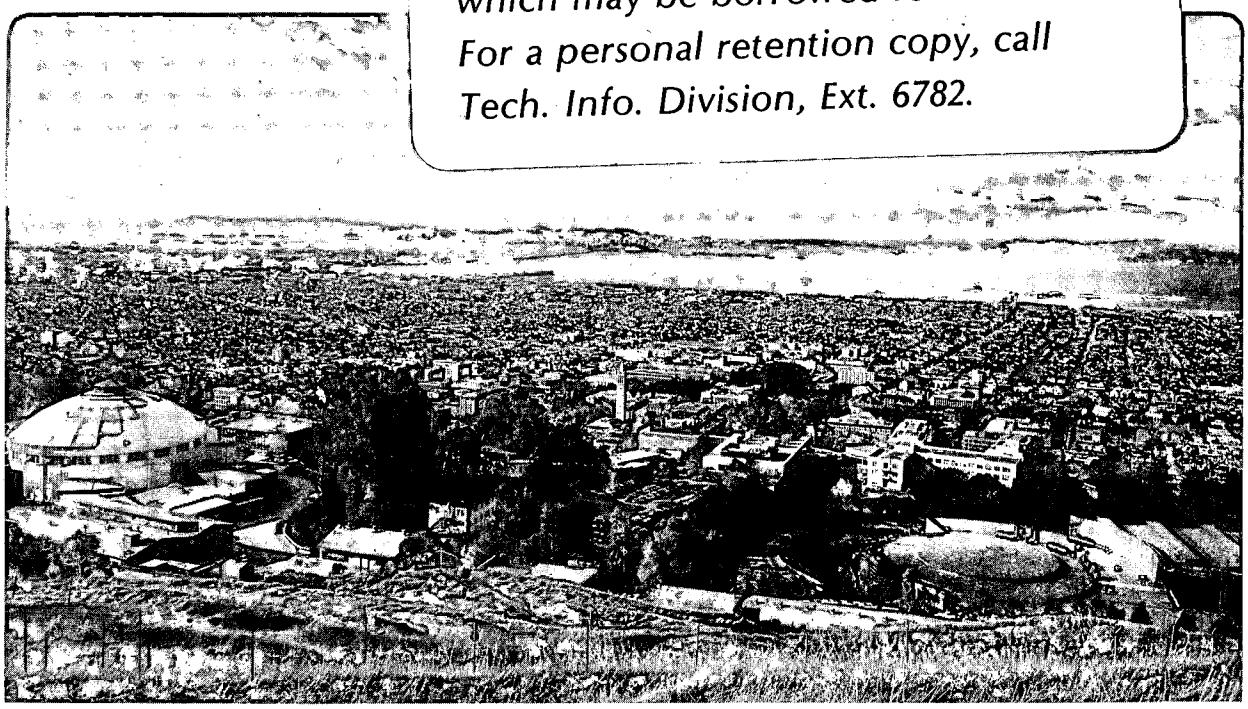

Prepared for the U.S. Department of Energy under Contract DE-AC03-76SF00098

DISCLAIMER

VELOCITY PLOTS AND CAPTURE ZONES OF PUMPING CENTERS FOR GROUND WATER INVESTIGATIONS

Joseph F. Keely[1] and Chin Fu Tsang[2]

ABSTRACT

Nonpumping monitoring wells are commonly installed and sampled to delineate the extent of a contaminant plume and its chemical character. Samples from municipal and private pumping wells are frequently collected during ground water contamination investigations as well. Pumping wells are also employed for remedial actions.

To properly interpret sampling data from monitoring and pumping wells and to estimate their potential effectiveness in remedial actions, it is important to clearly define the geometry of that portion of the aquifer contributing water to the well (the capture zone). Velocity distribution plots by manual and computerized methods are illustrated and shown to be simple and of reasonable accuracy.

[1] Ground Water Research Branch, R. S. Kerr Environmental Research Laboratory, U. S. Environmental Protection Agency.

[2] Senior Staff Scientist, Earth Sciences Divison, Lawrence Berkeley Laboratory, University of California, Berkeley, California.

INTRODUCTION

Oftentimes in the course of ground water investigations, water supply wells are sampled to obtain first-order approximations of the quality of water being delivered to consumers. The most common response to showings of unacceptable levels of contaminants is the installation of low cost, small diameter nonpumping monitoring wells for the express purpose of estimation of the magnitude and extent of the problem. The differences in construction, operation, and sampling of supply (pumping) wells as opposed to monitoring (nonpumping) wells may result in combined data sets which are confusing to the investigator. The primary exception, of course, is the case where the contaminant of concern has spread ubiquitously throughout the aquifer--a rare occurrence indeed.

Since very limited areal and vertical extent of contaminant plumes is the norm, combining data from wells of different construction and operation to produce contours of contaminant concentrations for source location or remedial action could potentially result in poor decisions, wasted funds, and so on. Unfortunately, such a predicament is all too often encountered. Several recent articles address these points in greater detail (Gibb and others, 1981; Keely, 1982; Keely and Wolf, 1983; Keith and others, 1983; Nacht, 1983; Schuller and others, 1981; and Schmidt, 1977 and 1982). In the present paper, it shall be assumed that data have been appropriately corrected to account for the different sources of data variability. Based on this, several easily mastered methods for rapid estimation of the impact of pumping centers on nearby contaminant plumes are described and illustrated by examples.

MANUAL PLOTS OF VELOCITY DISTRIBUTIONS

The velocity of flow through an aquifer can be simplistically represented by rearranging and slightly modifying Darcy's law, which is:

$$Q = KIA,$$

where

Q is the volumetric flow rate in gallons per day
(metric: cubic meters/day),

K is the hydraulic conductivity in gallons per day per square foot
(metric: meters per day),

I is the hydraulic gradient (dimensionless),

A is the cross-sectional area through which flow occurs in square feet
(metric: square meters).

By rearrangement alone, "Darcy velocity" (V_D) expressions are obtained:

$$\frac{Q}{A} = KI = V_D$$

But, since the flow actually occurs only through the pores, rather than through the entire cross-sectional area (A), a slight modification is needed. Division of the Darcy velocity by the effective porosity (ϕ_e) yields the true pore velocity (v).

$$\frac{Q}{A\phi_e} = \frac{KI}{\phi_e} = \frac{V_D}{\phi_e} = v$$

Generally one finds the left-hand term of the preceding relationship to be most useful for computing the velocity towards a pumping well because 'Q' is usually known for the well and 'A' is readily estimated. Assuming uniformly

radial flow towards the well is possible, the cross-sectional area (A) through which flow must pass to reach the well is equal to the area of the curved face of an imaginary cylinder of radius 'r'. That radius is chosen by the investigator as the distance from the well where the velocity effect is of interest to him or her, and is entirely arbitrary. The area of the curved face of the imaginary cylinder at that radial distance is given by $A = 2\pi rh$ where 'h' is the height of the imaginary cylinder (the effective saturated thickness of the aquifer zone yielding water to the well). Naturally this implies that there is a <u>distribution</u> of velocities surrounding the pumping well, which increase in magnitude as one gets closer and closer to the well. By substitution of $A = 2\pi rh$ into the velocity equation $Q \div A\phi_e = v$, one arrives at the operative formula needed: $Q \div 2\pi rh\phi_e = v_{pumping}$.

The right-hand term of the pore velocity form of Darcy's law is generally employed for estimation of the natural flow velocity, $KI \div \phi_e = v_{natural}$. This is because the average hydraulic conductivity (K) and hydraulic gradient (I) are usually known or fairly well estimated for an aquifer, whereas the average bulk flow (Q) and cross-sectional area (A) of the aquifer are not usually known or estimated accurately. One must estimate the effective porosity (ϕ_e) regardless of the approach adopted.

These simple formulae for $v_{pumping}$ and $v_{natural}$ are quite often all that can be justifiably employed because detailed information on variations in hydraulic conductivity, flow, hydraulic gradient, and so forth are unavailable to the investigator--at least in the initial stages of a contaminant investigation.

Manual plots of the velocity distribution surrounding a pumping well, in the presence of a real natural flow rate and direction, can be readily constructed with the equations just described. The data in Table 1 result from such an approach; also incorporated in Table 1 is a column listing the theoretical drawdown, calculated by use of a hand-held programmable calculator version of the Theis equation (Warner and Yow, 1979). The important features of the data in Table 1 are that velocities from natural flow and pumpage are added together to yield net velocities at distances upgradient of the well, whereas their differences must be obtained to yield net velocities downgradient of the well. This is quite sensible since the natural flow system is moving waters toward the well on the upgradient side of the well, but is trying to move waters away from the well on its downgradient side. Figure 1 is a graphical presentation of the data in Table 1, to facilitate conceptual appreciation of this discussion.

As can be seen in Figure 1 and Table 1, at some distance downgradient the pull of waters back toward the well by pumping is exactly countered by the flow away from the well due to the natural flow velocity. Todd (1980) refers to this as the "stagnation point"; the American Petroleum Institute (1972) refers to it as a "velocity divide". Note that the stagnation point/velocity divide occurs well within the cone of depression caused by pumping. This may seem counterintuitive initially, but calculation of net water surface elevations (by subtraction of drawdown values from prepumping elevations) will confirm that the situation depicted is quite real. This relationship is such that the greater the pumping stress, the farther downgradient the velocity divide

Table 1. Drawdowns and Velocities Toward a Well Constantly Discharging 500 Gallons per Minute (114 m^3/hr) for 1000 Minutes.

Observation Radius (feet)	Theoretical Drawdown (feet)	Velocity Due to Pumping (feet/day)	Net Velocity Upgradient (feet/day)	Net Velocity Downgradient (feet/day)
25	1.19	20.44	23.33	17.55
50	1.04	10.22	13.11	7.33
75	0.94	6.81	9.70	3.92
100	0.88	5.11	8.00	2.22
125	0.83	4.09	6.98	1.20
150	0.78	3.14	6.03	0.25
175	0.75	2.92	5.81	0.03
200	0.72	2.55	5.44	-0.34
225	0.69	2.27	5.16	-0.62
250	0.67	2.04	4.93	-0.85
275	0.65	1.86	4.75	-1.03
300	0.62	1.70	4.59	-1.19
325	0.61	1.57	4.46	-1.32
350	0.59	1.46	4.35	-1.43
375	0.57	1.36	4.25	-1.53
400	0.56	1.28	4.17	-1.61
425	0.55	1.20	4.09	-1.69
450	0.53	1.14	4.03	-1.75
475	0.52	1.08	3.97	-1.81
500	0.51	1.02	3.91	-1.87
⋮	⋮	⋮	⋮	⋮
750	0.42	0.68	3.57	-2.21
⋮	⋮	⋮	⋮	⋮
1000	0.35	0.51	3.40	-2.38

Notes: T is transmissivity (=5 x 10^5 gallons/day/foot), S is the storage coefficient (=0.005), h is the saturated aquifer thickness (= 100 feet), ϕ_e is the effective porosity (= 0.30), and I is the natural gradient (= 0.0013, or 13 feet per ten thousand feet; a water level elevation change of roughly 8 feet per mile). Positive velocity values indicate flow toward the well. Negative velocities indicate flow away from the well. Also note: m = feet x 0.31,
m^3 = gallons x 0.21
km = miles x 1.62

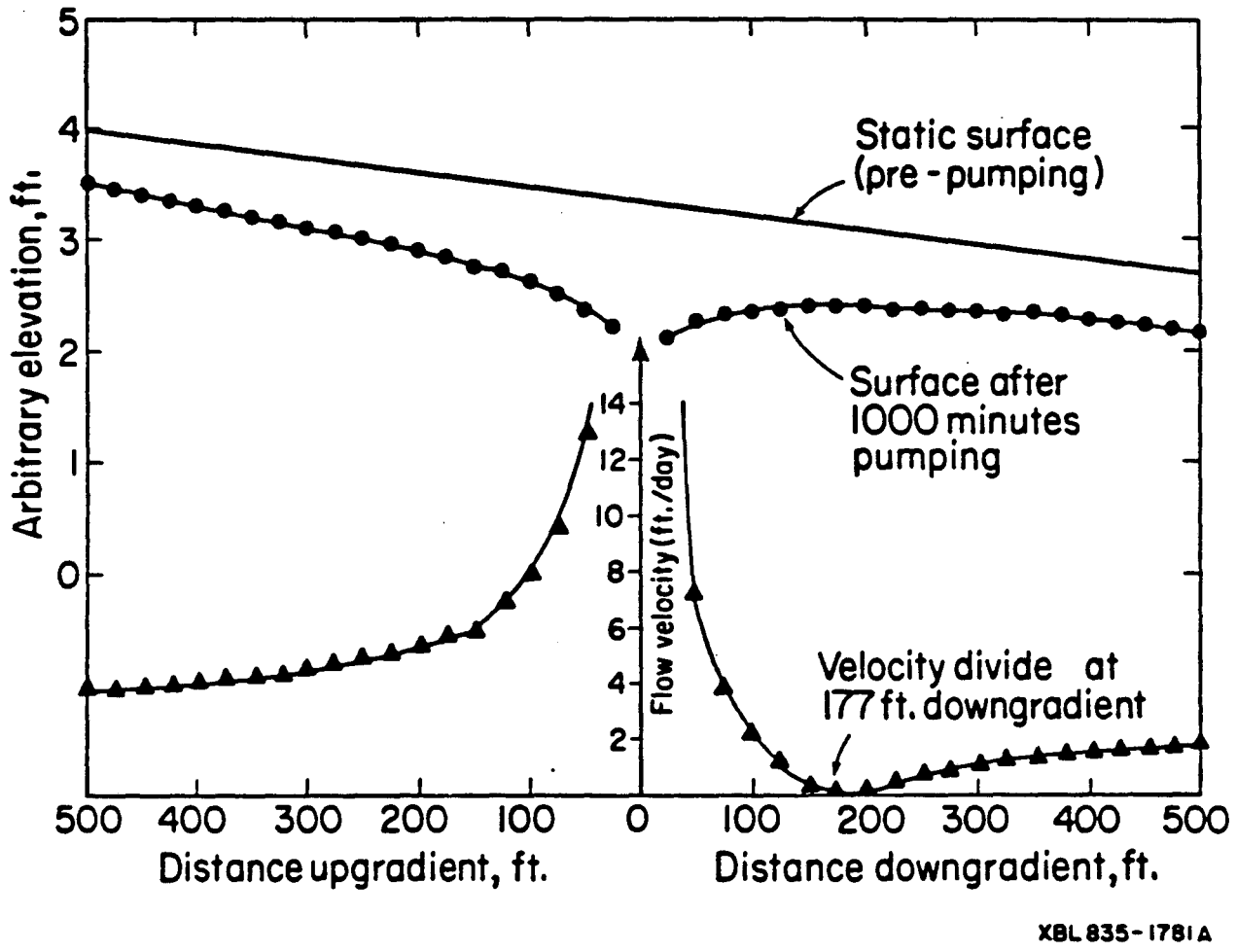

Figure 1. Drawdown and velocity distribution plot for data presented in Table 1.

occurs (for a given natural flow velocity). Conversely, the greater the natural flow velocity, the closer the divide comes to the pumping well (for a given pumping stress).

It is much more efficient to solve directly for the distance to the stagnation point than it is to construct plots like Figure 1. One abides by the definition of the stagnation point and sets the expression for $v_{pumping}$ equal to the value of $v_{natural}$:

$$v_{pumping} = v_{natural} \qquad \text{(definition of stagnation)}$$

$$Q \div 2\pi r h \phi_e = v_{natural} \qquad \text{(substitution)}$$

and then one rearranges this to solve directly for r:

$$r = Q \div 2\pi h \phi_e v_{natural}.$$

Using the data from Table 1 (for the graphical comparison see Figure 1),

$$r = 9.63 \times 10^4 \text{ ft}^3/\text{day} \div 2\pi(100 \text{ ft})(0.30)(2.895 \text{ ft/day})$$

$$= 176.5 \text{ ft} \quad (\text{metric: } 53.8 \text{ m}).$$

Todd (1980) notes that the maximum width of the upgradient inflow zone is equal to 2π times the stagnation distance immediately downgradient. Hence, contaminated waters lying just beyond π times the stagnation distance (π x 176.5 ft = 554 ft (169 m) for the preceding example) to either side of the well are <u>not</u> drawn into the well. Again, this occurs despite the fact that significant drawdowns are felt there (0.5 ft (15 cm) in Table 1). These boundaries define the areal limits of what will be referred to as the "capture zone" of the well. Only for the extremely rare case of zero natural flow velocity are the areal boundaries of the capture zone and the cone of depression everywhere identical.

The importance of performing these calculations can hardly be overemphasized for ground water contamination investigations. Using such calculations it is no great task to show that a line of wells designed to stop the advance of a contaminant plume due to a fairly large natural flow velocity may fail miserably, despite the fact that their adjacent cones of depression overlap (an almost sacred benchmark for field practitioners). Figure 2 illustrates such a situation, using selected data from Table 1.

It is also important to note that this is not an earth-shattering discovery. Virtually all contaminant transport codes are based on the calculation of a velocity field; so that use of such codes need not be viewed with suspicion from that standpoint. However, it is the authors' contention that because the vast majority of ground water contamination investigations are initiated, performed, and concluded without the use of numerical transport models and qualitative decision benchmarks such as "overlapping cones of depression" are heavily employed, it is imperative that velocity plots now be emphasized.

RADIAL FLOW TIME-SERIES MODEL (RT)

Major impediments to the widespread use of sophisticated contaminant transport models include their general reliance on advanced mathematics, the need for large computing systems and programming skills, and the tedious selection and construction of appropriate grids. In order to circumvent the most undesireable of these characteristics, two nondispersive transport codes are presented here which rely on the simple velocity expression discussed in the preceding section. The examples employed here to illustrate these codes were produced with very short FORTRAN programs, which are currently available from

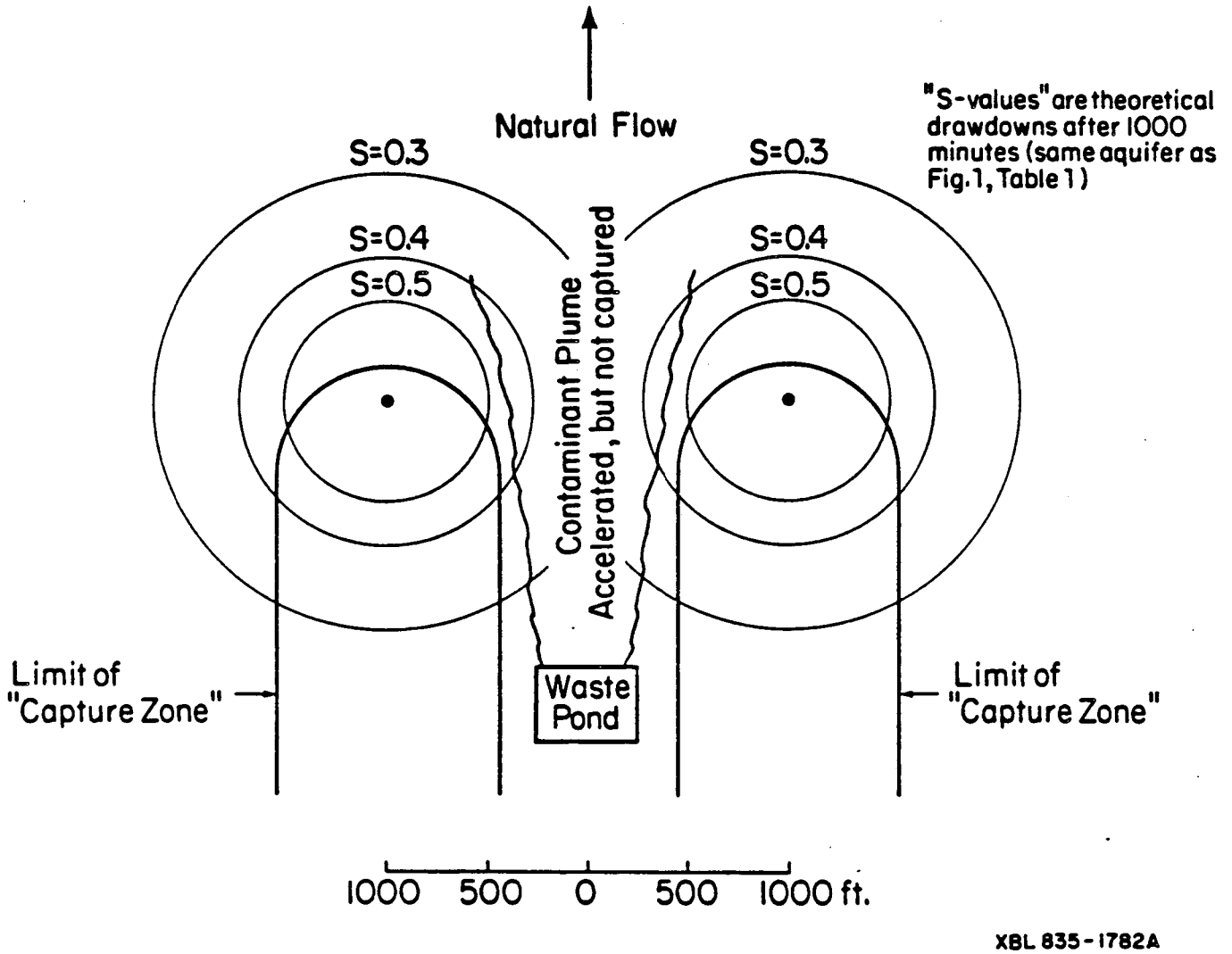

Figure 2. Two wells accelerating a plume without capturing it.

the authors. The full program descriptions, expanded theory, and users guides will be released shortly as part of a report by Lawrence Berkeley Laboratory (Javandel and others, 1983a). Also of great interest to field personnel may be the planned subsequent release of hand-held programmable calculator and microcomputer versions of these same codes (Javandel and others, 1983b).

The radial flow time-series model, RT, is particularly useful for estimation of impacts to a pumping well from nearby contaminant sources. Since this code ignores regional flow, it is not as detailed as might be required for many complete analyses, but its simplicity and brevity make it attractive for rapid estimation purposes (RESSQ, the other code to be described below, incorporates regional flow). One may use RT with confidence for such situations as the combination of a large pumping well and a low regional (natural) flow velocity. Caution must be exercised when using RT for field problems where low pumping stresses are combined with fairly rapid natural flows because substantial errors may result. RT is capable of providing several useful plots:

(1) time-concentration data,

(2) radial distance-concentration data,

(3) specified point (x, y)-concentration data, and

(4) selected concentration contours.

The primary situation examined here by RT is one where a pumping well is surrounded by several observation wells, some of which are being impacted by a spreading contaminant plume. Of great interest are the changes in levels of contaminants at the observation wells and the pumping well as pumping progresses; these concentration-time patterns will yield substantial clues as to

the spatial distribution of the contaminants. This technique of correlating time-series data to spatial distributions has been developed from the techniques described by Keely (1982).

Because of the radial flow situation addressed by RT, it is useful to slightly modify the expression for $v_{pumping}$ given earlier. In radial coordinates, it is:

$$v_{pumping} = v_{radial} + v_{theta} = v_r + v_\theta,$$

where v_r and v_θ are the radial and angular components of velocity in the radial coordinate system (r, θ), analogous to the x and y velocity components of the Cartesian system (x, y). Substitution of the expression for $v_{pumping}$ then gives:

$$v_{pumping} = \frac{Q}{2\pi r h \phi_e} = v_r + v_\theta$$

For a pumping well at the origin (0, 0) of the plot to be constructed, $v_\theta = 0$ by symmetry, so $v_{pumping} = v_r$. Hence, the expression for v_r at some radial distance (r) from the pumping well in radial coordinates is the same as $v_{pumping}$ calculated previously by considering the distance to the edge of an imaginary cylinder around the well:

$$v_r = \frac{Q}{2\pi r h \phi_e} .$$

Recognizing that the velocity on some radial (v_r) is the result of the change in distance being divided by the change in time (dr/dt), a substitution can be made

$$v_r = \frac{dr}{dt} = \frac{Q}{2\pi r h \phi_e}$$

which will lead directly to the equations most useful for estimating the position of the contaminant front. Solution of the differential expression $dr/dt = Q \div 2\pi rh\phi_e$ requires only the most straightforward rules of integration; (1) that constants in the equation are unaffected, (2) that open integrals imply simple subtraction of the maximum and minimum values (in this case, the time of interest minus some arbitrary starting time of pumping, or $t - t_o$), and (3) that a variable (here, radial distance) is raised to the next power and divided by a value equal to that power (e.g., 'r' becomes $r^2 \div 2$). Hence, integration of the radial velocity expression gives:

$$\frac{\frac{r^2}{2} - \frac{r_0^2}{2}}{(t - t_0)} = \frac{Q}{2\pi h\phi_e} .$$

This can be readily rearranged to solve for the distance traveled during a specific time ($= t - t_0$),

$$r = \left[r_0^2 + \frac{Q(t - t_0)}{\pi h\phi_e} \right]^{1/2} .$$

Likewise, it can be rearranged to solve for the time required to travel a specific distance ($= r - r_0$),

$$t = t_0 + \frac{(r^2 - r_0^2)\pi h\phi_e}{Q}$$

These two equations form the basis for calculations performed by RT.

For example, if an observation well is located at a distance r_1 from the pumping well, then a time series of contaminant concentration measurements at that well taken at t_1, t_2, t_3, ..., t_n, will yield the corresponding locations

of r_2, r_3, ..., r_{n+1} for those concentrations at any given time. Hence, assuming that the concentration distribution of a given solute in an aquifer is not uniform, the time-series data from a given well can be mapped out into the aquifer to produce a "snapshot" of the spatial contaminant concentration distribution, along the radius between the observation well and the production well at various times. By using observation wells in several directions from the pumping well, an areal picture of the contaminant concentration in the aquifer at various times can be determined.

To illustrate this situation, RT was used to create the sequence of plots shown in Figure 3, which run from prepumping to a little more than one day's pumping. Each of the scatter points is brought closer to the origin (0, 0) by the pumping well located there. Alternatively, RT can be used to generate contours of relative concentration, such as shown in Figure 4.

Perhaps the most powerful outputs generated by RT, however, are the individual relative concentration-time plots for any of the six monitoring/observation wells or the pumping well (Figure 5). It should come as no surprise that these patterns of contaminant arrival look like the breakthrough curves generated during tracer experiments; the fundamental laws and the field design are the same. The noticeable difference is that the low level leading edge is absent from the early time portions of the plots because dispersive effects are not accounted for by RT.

An invaluable variation on this presentation of relative concentration-time plots is also output by RT (Figure 6). Relative concentrations are plotted versus distance for a select number of times of interest, generating a

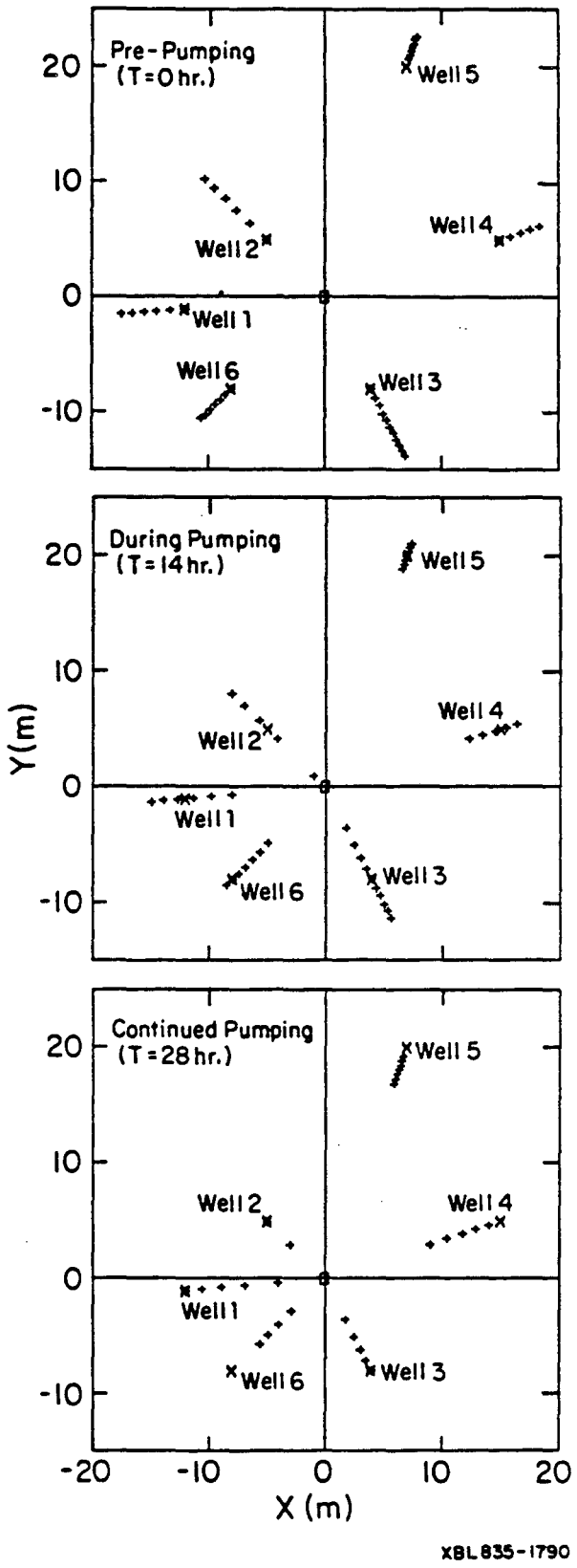

Figure 3. Scatter maps produced by radial draw-time series model.

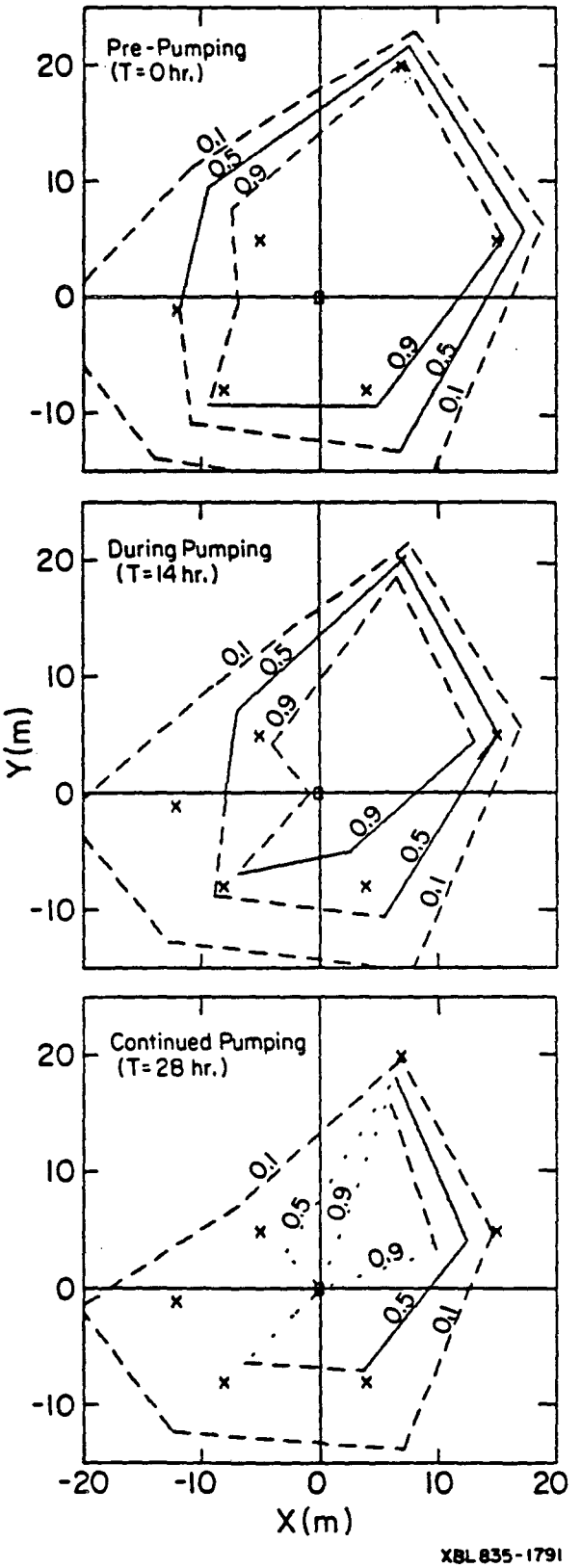

Figure 4. Contour maps produced by radial draw-time series model.

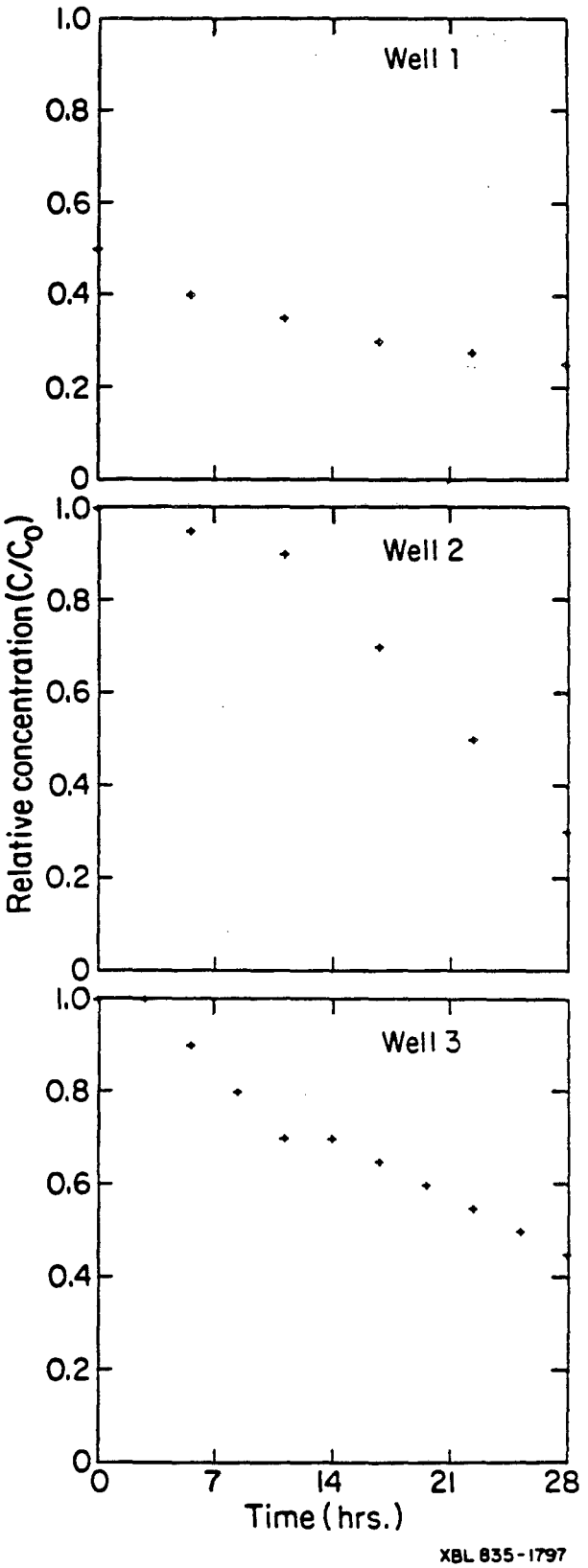

Figure 5. Relative concentrations versus time of pumpage plots produced by radial draw-time series model.

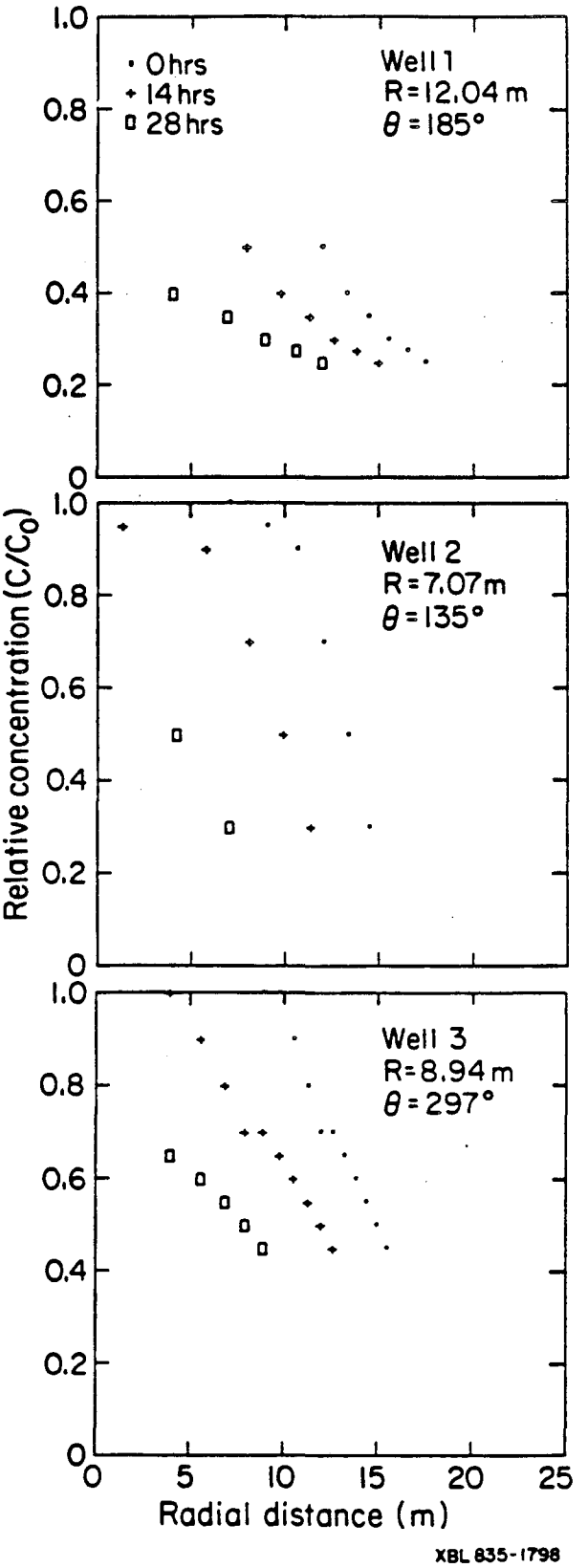

Figure 6. Relative concentrations along selected radials without attenuation (R = 1.0).

family of curves. Thus one can examine the relative concentration along a selected radial and readily observe the manner in which this relationship changes with time. In the example shown in Figure 6, it can be seen that the farther from the pumping well, the less the disturbance of the contaminant plume. As one gets closer to the pumping well, the greater the disturbance, so that the overall relative concentrations are lowered rapidly and the length of the plume expands considerably. This kind of graphical presentation underscores the need to plot velocity distributions to estimate the impact of pumping centers on plume movement. Plume travel times based solely on a single average velocity will be much greater than they ought to be, giving planners a false sense of security or lack of urgency.

Because of retardation/attenuation or degradation of some contaminants by physical, chemical, or biological interactions, the velocity at which a contaminant species is transported through the subsurface may be substantially less than the average pore water velocity. Since the magnitude of these effects can rarely be assessed in detail, use of an empirical weighting factor is often justified. A simplified retardation factor (R) can be incorporated into velocity calculations of the water front movement (v_r) to give the velocity of the contaminant (v_c):

$$v_c = v_r/R$$

where one notes that R is equal to the ratio of the average pore water velocity to the contaminant velocity ($R = v_r/v_c$). Use of a large retardation factor ($R \gg 1$) then implies considerable attenuation of the contaminant relative to the water front. Figure 7 is a replotting of the example in Figure 6, but with R = 1.5.

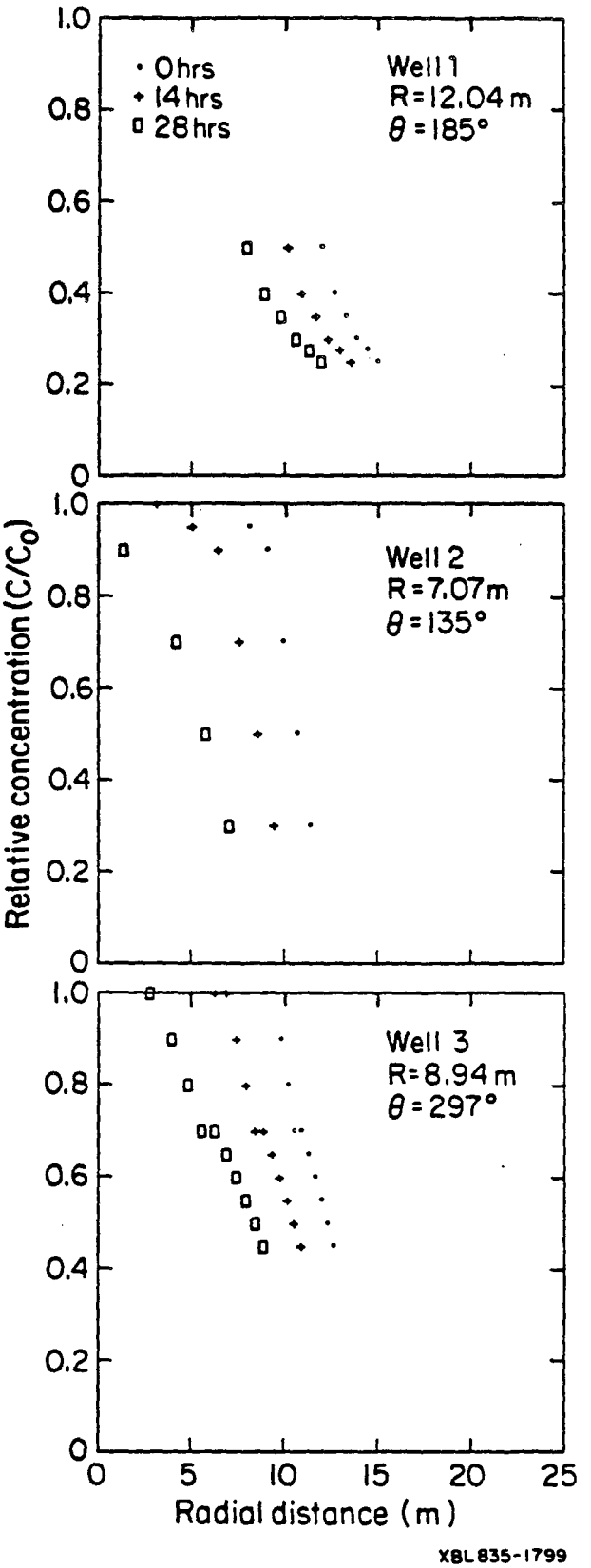

Figure 7. Relative concentrations along selected radials with attenuation (R = 1.5).

RESSQ MODEL

While the brevity and simplicity of RT make it a useful tool for rapid assessment of simplified situations, it does lack the ability to deal with the effect on contaminant levels at pumping and observation wells which is due to the regional/natural flow velocity. As was shown in the earlier section of this paper which described manual plotting techniques for velocity distributions, the effect of a moderate natural flow velocity can be quite important.

RESSQ is an expanded version of RT, capable of incorporating the natural flow velocity and also capable of simulating more complex situations where several pumping wells and contaminant sources need to be evaluated simultaneously. As such, it has been constructed so that all inputs and outputs are geared to a Cartesian (x, y) coordinate system (see Figure 8). The expression for velocity due to a pumping well was given previously as

$$v_r = \frac{Q}{2\pi r h \phi_e}$$

where r was the distance from the origin (0, 0) to the edge of an imaginary cylinder surrounding the well (radial flow assumption). It is useful to create a more generalized expression in terms of actual x- and y-coordinates. The easiest approach is to use the origin (0, 0) as a reference point and employ the Pythagorean theorem of geometry for right triangles,

$$r^2 = x^2 + y^2.$$

Here, the right triangle has its short sides parallel to the x- and y-axes, and its hypotenuse (of length r) defining the line connecting the origin (0, 0) to the point of interest (x, y). For a pumping well located at (x_0, y_0), the

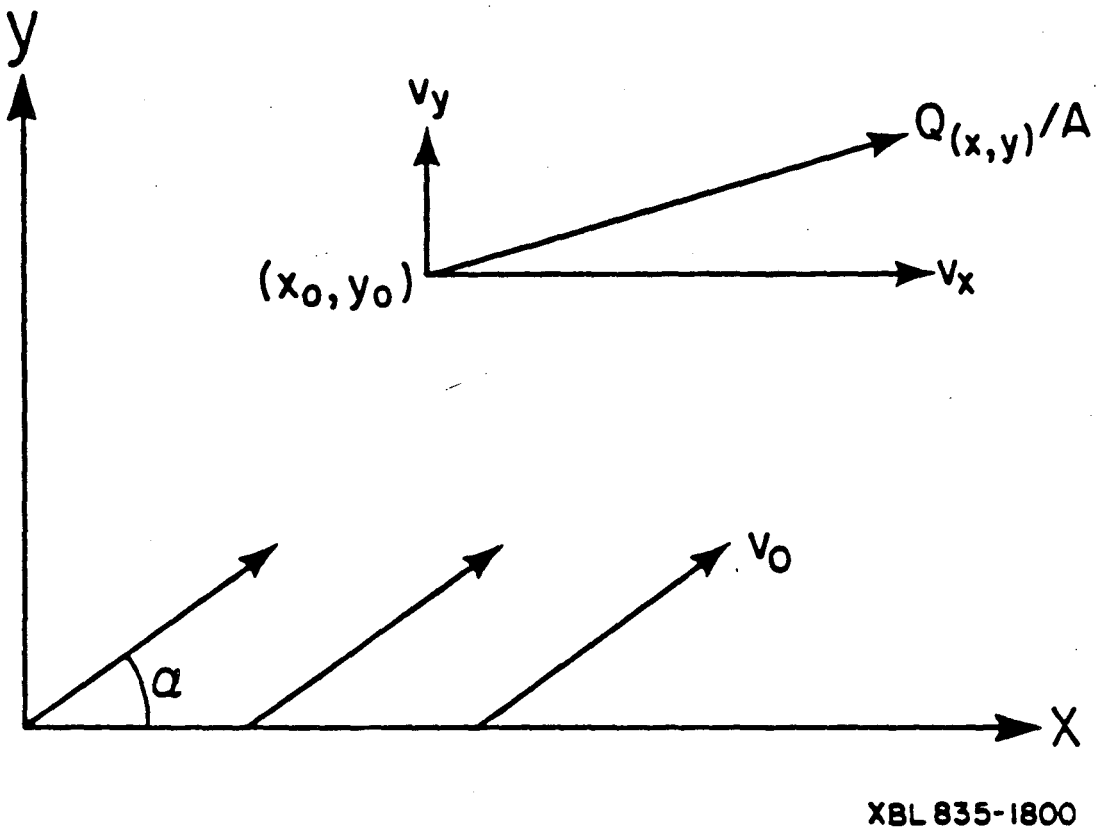

Figure 8. Cartesian system showing x- and y-components of pumping flow velocity and showing regional flow velocity with angle α to x-axis.

pumping velocity at the point of interest (x, y) has x- and y-components given by:

$$v_x = \frac{Q}{2\pi h \phi_e} \frac{x - x_0}{(x - x_0)^2 + (y - y_0)^2},$$

and

$$v_y = \frac{Q}{2\pi h \phi_e} \frac{y - y_0}{(x - x_0)^2 + (y - y_0)^2}.$$

The x and y components of the natural flow velocity v_0, which has a direction at an angle α from the x-axis, are: $v_x = v_0 \cos\alpha$, and $v_y = v_0 \sin\alpha$. If one considers a wastewater injection well (with $Q = 50\ m^3/hr$ or 220 gpm) located at point A in Figure 9 which is suspected of potentially contaminating a water supply well (also with $Q = 50\ m^3/hr$ or 220 gpm) located 848.5 m (2784 ft) away at point B, the prime questions to be answered are:

(1) What do the flow patterns of the system look like?

(2) Where will the injected wastewater front be after certain time periods (e.g., 0.5, 2, and 4 years)?

(3) How long does it take for the injected wastewater to reach the water supply well?

and

(4) How does the contaminant concentration vary at the water supply well?

Based on local geology, it has been estimated that the effective porosity (ϕ_e) of the aquifer is twenty five percent (25%).

As a first cut, analogous to the simple approach in RT, the regional/natural flow velocity will be neglected. Using RESSQ, Tables 2 and 3 are

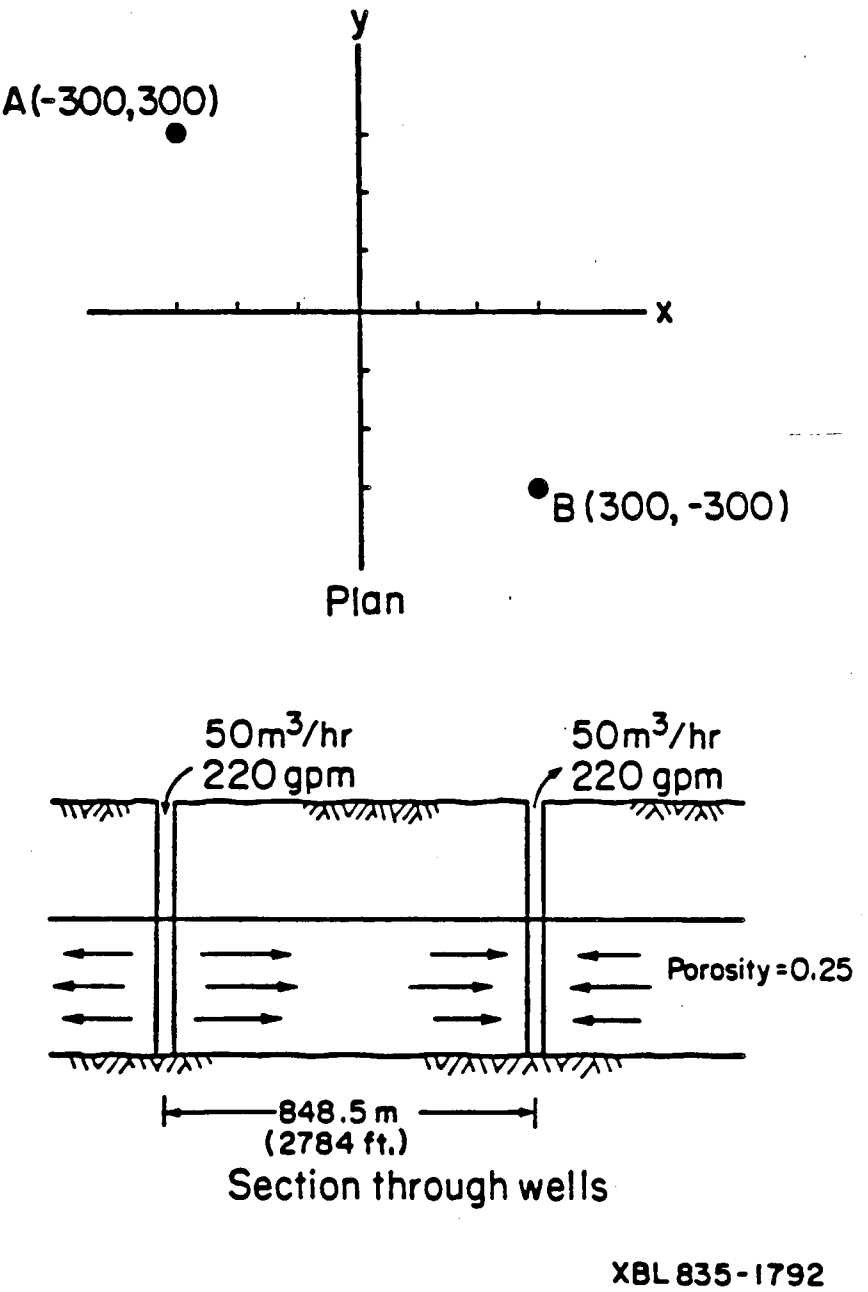

Figure 9. Plan view and cross section for RESSQ model examples (discussed in text).

Table 2. Streamlines Departing from Injection Well at Point A.

Number of the Line	Well Reached	Time of Arrival	Minimum Step in Cm.	Angle Beta in Degrees
1st	Prod. One	5.6 years	42.4264E+01	0.
2nd	Prod. One	6.2 years	42.4264E+01	8.0
3rd	Prod. One	7.0 years	42.4264E+01	16.0
4th	Prod. One	8.1 years	42.4264E+01	24.0
5th	Prod. One	9.5 years	84.8528E+01	32.0
6th	Prod. One	11.6 years	42.4264E+01	40.0
7th	Prod. One	14.4 years	42.4264E+01	48.0
8th	Prod. One	18.5 years	42.4264E+01	56.0
9th	Prod. One	24.6 years	42.4264E+01	64.0
10th	Prod. One	34.3 years	42.4264E+01	72.0
11th	Prod. One	50.4 years	42.4264E+01	80.0
12th	Prod. One	79.3 years	42.4264E+01	88.0
13th	Prod. One	137.0 years	42.4264E+01	96.0
14th	++++None+	200.1 years	84.8528E+01	104.0
15th	++++None+	200.8 years	84.8528E+01	112.0
16th	++++None+	201.3 years	84.8528E+01	120.0
17th	++++None+	200.8 years	84.8528E+01	128.0
18th	++++None+	201.7 years	84.8528E+01	136.0
19th	++++None+	201.5 years	84.8528E+01	144.0
20th	++++None+	201.4 years	84.8528E+01	152.0
21st	++++None+	200.1 years	84.8528E+01	160.0
22nd	++++None+	200.0 years	84.8528E+01	168.0
23rd	Prod. One	118.3 years	42.4264E+01	176.0
24th	Prod. One	70.3 years	42.4264E+01	184.0
25th	Prod. One	45.5 years	42.4264E+01	192.0
26th	Prod. One	31.4 years	42.4264E+01	200.0
27th	Prod. One	22.8 years	42.4264E+01	208.0
28th	Prod. One	17.3 years	42.4264E+01	216.0
29th	Prod. One	13.6 years	42.4264E+01	224.0
30th	Prod. One	11.0 years	42.4264E+01	232.0
31st	Prod. One	9.1 years	42.4264E+01	240.0
32nd	Prod. One	7.8 years	42.4264E+01	248.0
33rd	Prod. One	6.8 years	42.4264E+01	256.0
34th	Prod. One	6.0 years	84.8528E+01	264.0
35th	Prod. One	5.4 years	42.4264E+01	272.0
36th	Prod. One	5.0 years	42.4264E+01	280.0
37th	Prod. One	4.7 years	84.8528E+01	288.0
38th	Prod. One	4.5 years	84.8528E+01	296.0
39th	Prod. One	4.4 years	84.8528E+01	304.0
40th	Prod. One	4.3 years	42.4264E+01	312.0
41st	Prod. One	4.3 years	42.4264E+01	320.0
42nd	Prod. One	4.4 years	84.8528E+01	328.0
43rd	Prod. One	4.5 years	42.4264E+01	336.0
44th	Prod. One	4.8 years	42.4264E+01	344.0
45th	Prod. One	5.1 years	42.4264E+01	352.0

Table 3. Evolution of Concentration for Pumping Well at Point B.

Time in Years	Concentration In Percent	(C-CO)/(CD-CO)
4.303E+00	2.222	.0222
4.312E+00	4.444	.0444
4.364E+00	6.667	.0667
4.391E+00	8.889	.0889
4.499E+00	11.111	.1111
4.545E+00	13.333	.1333
4.714E+00	15.556	.1556
4.782E+00	17.778	.1778
5.024E+00	20.000	.2000
5.119E+00	22.222	.2222
5.448E+00	24.444	.2444
5.575E+00	26.667	.2667
6.016E+00	28.889	.2889
6.185E+00	31.111	.3111
6.771E+00	33.333	.3333
6.996E+00	35.556	.3556
7.778E+00	37.778	.3778
8.080E+00	40.000	.4000
9.135E+00	42.222	.4222
9.544E+00	44.444	.4444
1.099E+01	46.667	.4667
1.156E+01	48.889	.4889
1.358E+01	51.111	.5111
1.438E+01	53.333	.5333
1.730E+01	55.556	.5556
1.848E+01	57.778	.5778
2.283E+01	60.000	.6000
2.463E+01	62.222	.6222
3.142E+01	64.444	.6444
3.429E+01	66.667	.6667
4.550E+01	68.889	.6889
5.038E+01	71.111	.7111
7.028E+01	73.333	.7333
7.932E+01	75.556	.7556
1.183E+02	77.778	.7778
1.370E+02	80.000	.8000

generated. Table 2 lists the arrival times at the pumping well of the injected wastewaters flowing along streamlines between the two wells, depicted graphically by RESSQ in Figure 10. Note that nine of the streamlines carrying the contaminants have not reached the water supply well during the specified period of study which was arbitrarily chosen to be 200 years. The angle (β) at which each streamline leaves the injection well (relative to the x-axis) is also shown in Table 2. Note that streamlines 40 and 41 leave the injection well at angles of 312 and 320 degrees, respectively, and are the first to arrive at the water supply well--which agrees with one's intuitive expectations. The time of arrival of these two streamlines is 4.3 years; the water supply well is affected rather quickly in terms of a normal operational lifetime for the injection well (10-20 years).

Table 3 presents the time variation of concentration at the water supply well. Note that the total number of streamlines emanating from the injection well was again set at 45. Each of these streamlines represents 1/45 of the total injection rate, so mixing of the wastewater carried by each streamline with other unaffected waters drawn on by the water supply well increases the relative concentration of the wastewater contaminants by 1/45 or 2.22 percent. For the study period examined in this example, a maximum of 36 streamlines reach the water supply well from the wastewater injection well, resulting in a maximum relative concentration of 80 percent. Hence, if the injected wastewater was laden with 200 ppm of contaminant XXX, then 0.80 x 200 ppm = 160 ppm is the maximum concentration of contaminant XXX in the water discharged from the supply well. RESSQ is capable of presenting these data graphically, as

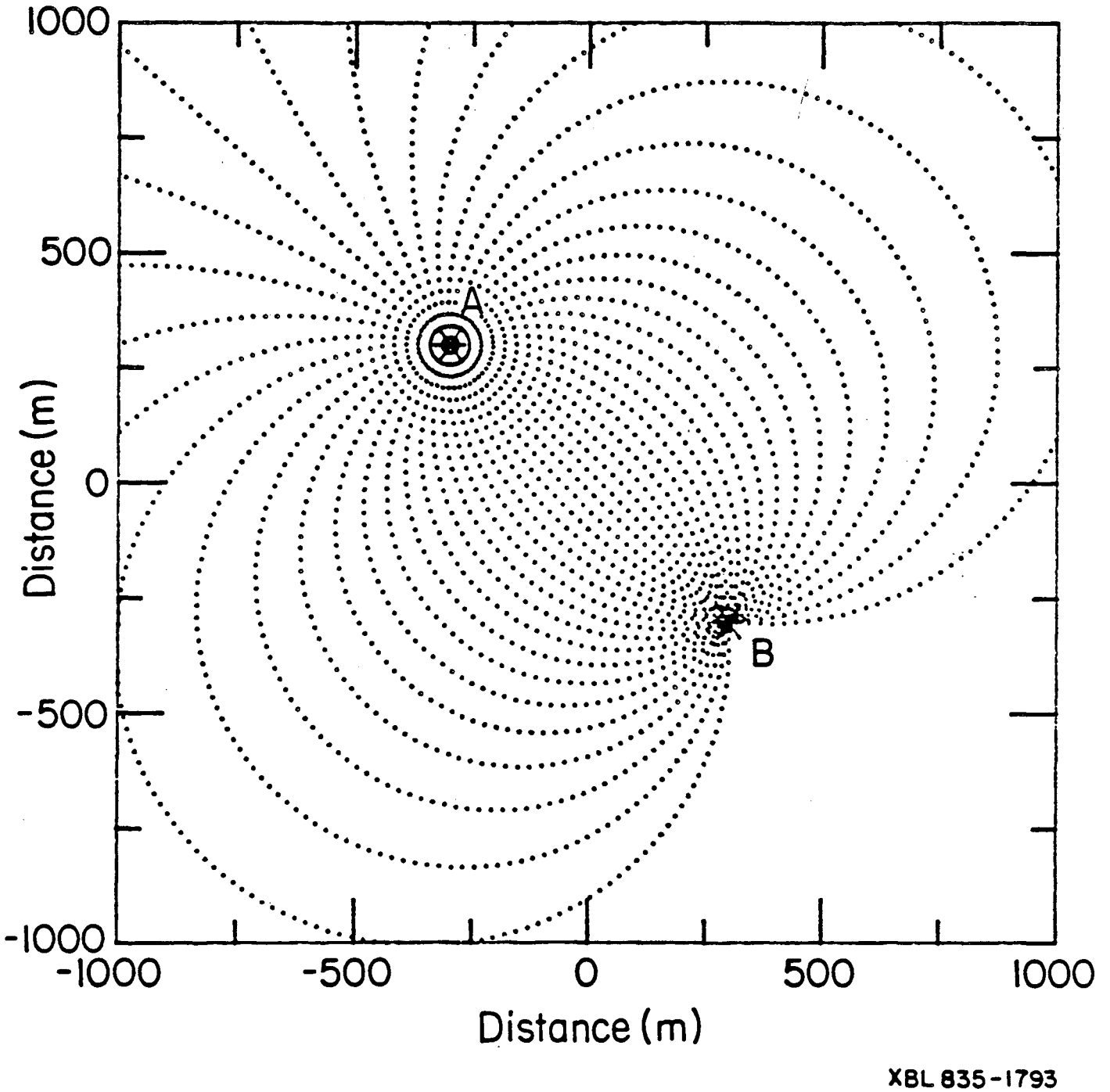

Figure 10. Streamlines for RESSQ model example without regional flow considered.

shown in Figure 11. Alternatively, RESSQ can be used to display selected contours, such as the position of the wastewater front after 0.5, 2, and 4 years, as shown in Figure 12.

The example just discussed can be expanded by using RESSQ to incorporate the effects of combining a regional/natural flow velocity of 50 m/year (0.45 ft/day) oriented perpendicular to a line joining the two wells (i.e., $\alpha = 45°$). Using the equations developed earlier, the x- and y-components of the natural velocity are, respectively,

$$v_x = v_0 \cos \alpha - \sum_{P=1}^{N} \frac{Q_p}{2\pi h \phi_e} \frac{(x - x_p)}{(x - x_p)^2 + (y - y_p)^2}$$

$$+ \sum_{i=1}^{M} \frac{Q_i}{2\pi h \phi_e} \frac{(x - x_i)}{(x - x_i)^2 + (y - y_i)^2},$$

and

$$v_y = v_0 \sin \alpha - \sum_{P=1}^{N} \frac{Q_p}{2\pi h \phi_e} \frac{(y - y_p)}{(x - x_p)^2 + (y - y_p)^2}$$

$$+ \sum_{i=1}^{M} \frac{Q_i}{2\pi h \phi_e} \frac{(y - y_i)}{(x - x_i)^2 + (y - y_i)^2},$$

For each equation, the first term represents the contribution of the regional flow velocity. The second term represents the sum of the contributions from the pumping well(s) and is a negative quantity because flow is being removed from the system. The remaining term is the sum of the contributions from the

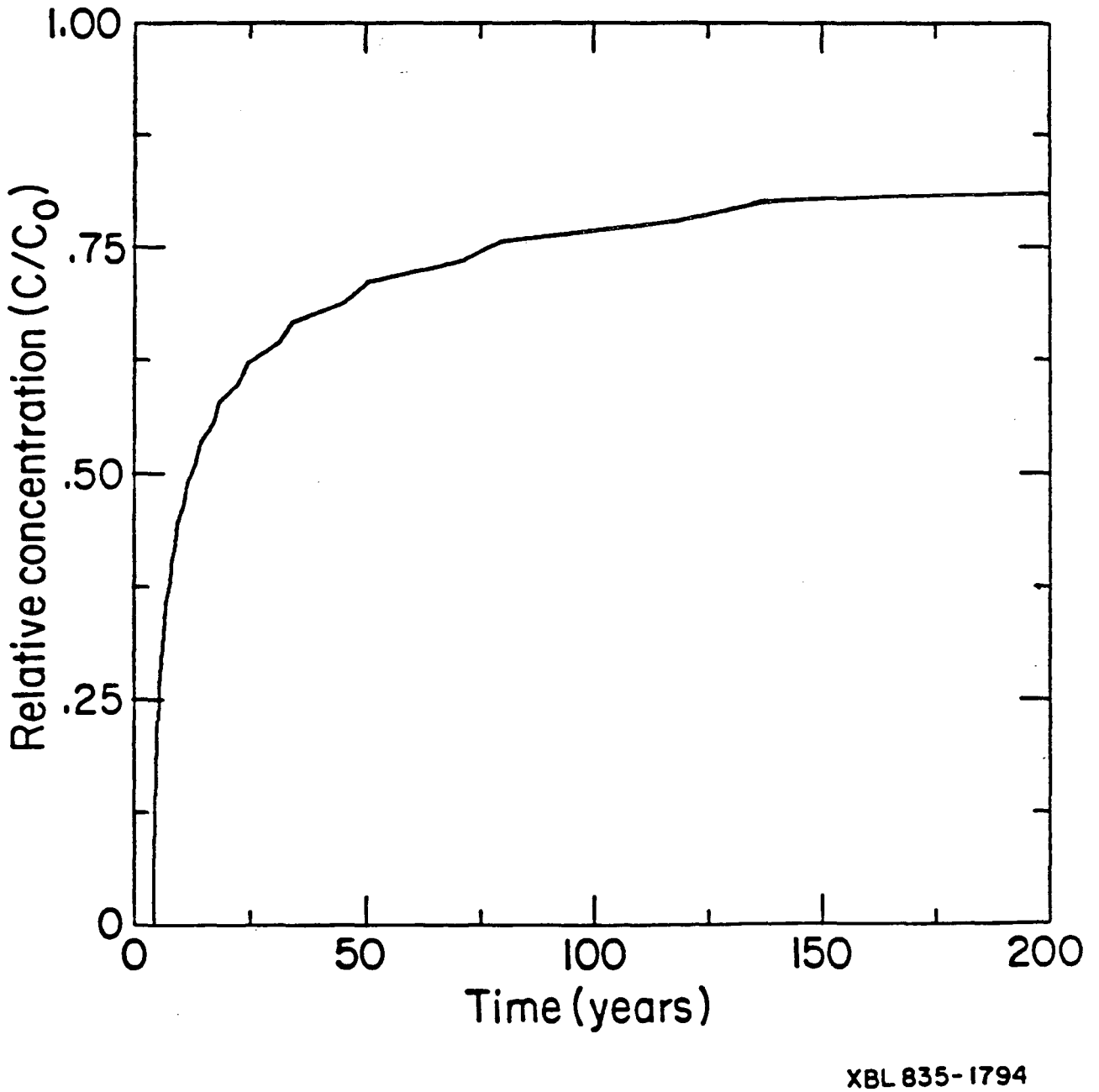

Figure 11. Time variation of relative concentration at water supply well without regional flow considered.

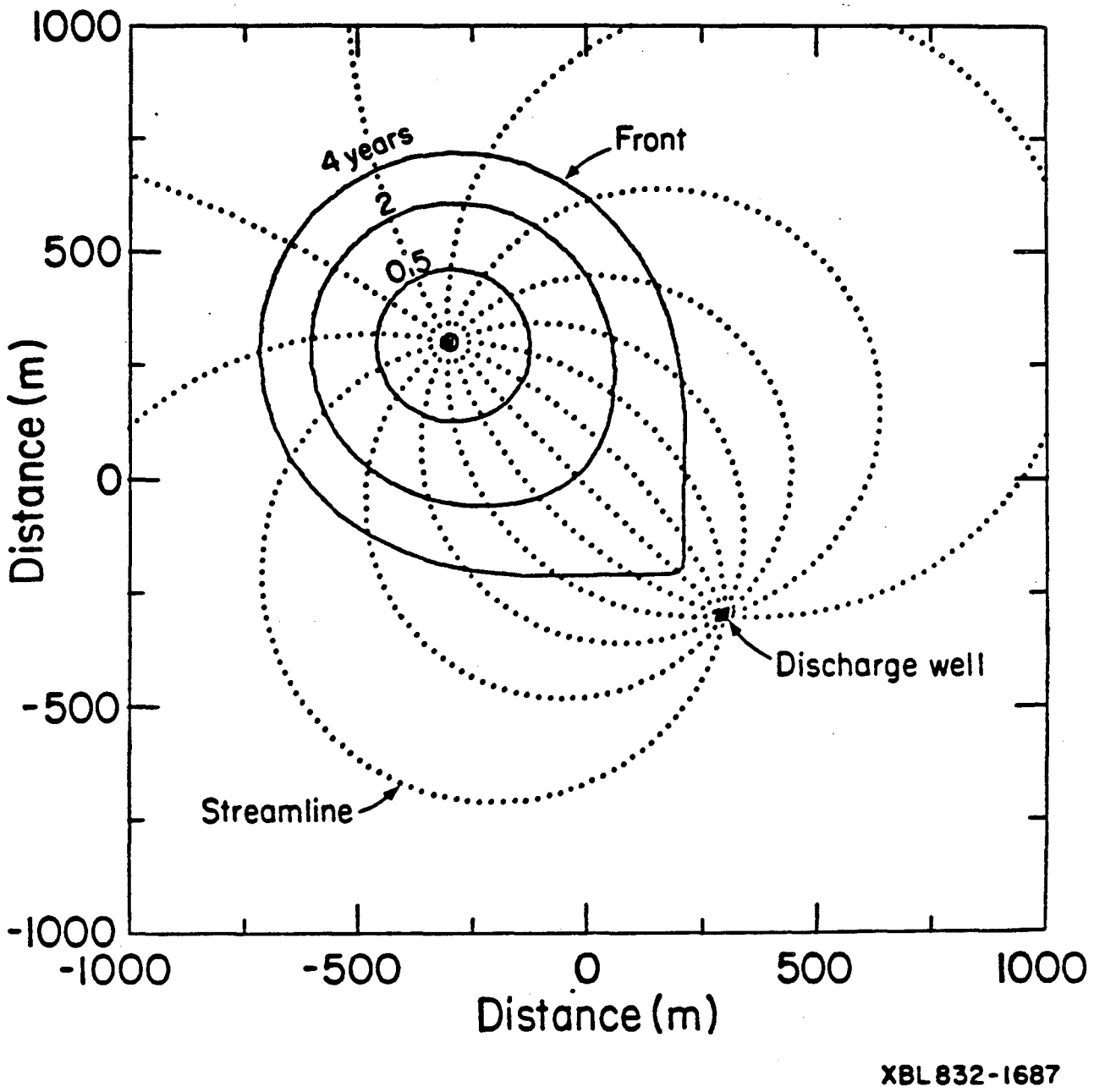

Figure 12. Position of injected wastewater front after 0.5, 2, and 4 years without regional flow considered.

injection well(s) and is a positive quantity because flow is being added to the system.

Using these equations, RESSQ generated Table 4, which presents the arrival times of the wastewater flowing along streamlines between the injection and supply wells, depicted graphically in Figure 13. Note that only 20 of the 45 streamlines emanating from the injection well are now able to reach the supply well. The remaining 26 are washed away by the regional/natural flow system. This causes the maximum relative concentrations (44 percent) of wastewater contaminants in the water discharged from the water supply well to be considerably lower (Figure 14) than was the case where regional flow was not considered (Figure 11).

The contours of the position of the wastewater front after 0.5, 2, and 4 years are also shown in Figure 13; it is quite evident that the regional flow has displaced the contours downgradient as compared with the earlier presentation neglecting regional flow (Figure 12). To some, this might tend to imply some mitigation of the urgency of the situation for the water supply well owner; however, one should note that the injected wastewater front arrives at 4.6 years (the 35th streamline, Table 4). This is not so different from the 4.3 years calculated in the discussion where regional flow was neglected. Hence, in this case, the regional flow is adequate to substantially reduce the contaminant loadings to the supply well, but it does not significantly affect the arrival time of the contaminant plume, despite the fact that the injection well is a healthy distance directly across the regional gradient from the pumping well.

Table 4. Streamlines Departing from Injection Well with Regional Flow.

Number of the Line	Well Reached	Time of Arrival	Minimum Step in Cm.	Angle Beta in Degrees
1st	++++None+	199.9 years	84.8528E+01	0.
2nd	++++None+	199.9 years	84.8528E+01	8.0
3rd	++++None+	200.0 years	84.8528E+01	16.0
4th	++++None+	200.0 years	84.8528E+01	24.0
5th	++++None+	199.9 years	84.8528E+01	32.0
6th	++++None+	200.0 years	84.8528E+01	40.0
7th	++++None+	199.9 years	84.8528E+01	48.0
8th	++++None+	200.0 years	84.8528E+01	56.0
9th	++++None+	199.9 years	84.8528E+01	64.0
10th	++++None+	199.9 years	84.8528E+01	72.0
11th	++++None+	199.9 years	84.8528E+01	80.0
12th	++++None+	200.0 years	84.8528E+01	80.0
13th	++++None+	199.9 years	84.8528E+01	96.0
14th	++++None+	199.9 years	84.8528E+01	104.0
15th	++++None+	199.9 years	84.8528E+01	112.0
16th	++++None+	200.0 years	84.8528E+01	120.0
17th	++++None+	199.9 years	84.8528E+01	128.0
18th	++++None+	200.0 years	84.8528E+01	136.0
19th	++++None+	200.0 years	84.8528E+01	144.0
20th	++++None+	199.9 years	84.8528E+01	152.0
21st	++++None+	200.0 years	84.8528E+01	160.0
22nd	++++None+	200.0 years	84.8528E+01	168.0
23rd	++++None+	199.9 years	42.4264E+01	176.0
24th	++++None+	199.9 years	42.4264E+01	184.0
25th	++++None+	200.0 years	42.4264E+01	192.0
26th	Prod. One	21.4 years	42.4264E+01	200.0
27th	Prod. One	11.6 years	42.4264E+01	208.0
28th	Prod. One	8.7 years	42.4264E+01	216.0
29th	Prod. One	7.1 years	42.4264E+01	224.0
30th	Prod. One	6.2 years	42.4264E+01	232.0
31st	Prod. One	5.5 years	42.4264E+01	240.0
32nd	Prod. One	5.1 years	42.4264E+01	248.0
33rd	Prod. One	4.8 years	42.4264E+01	256.0
34th	Prod. One	4.7 years	84.8528E+01	264.0
35th	Prod. One	4.6 years	42.4264E+01	272.0
36th	Prod. One	4.7 years	42.4264E+01	280.0
37th	Prod. One	4.8 years	84.8528E+01	288.0
38th	Prod. One	5.1 years	84.8528E+01	296.0
39th	Prod. One	5.5 years	84.8528E+01	304.0
40th	Prod. One	6.1 years	42.4264E+01	312.0
41st	Prod. One	7.0 years	42.4264E+01	320.0
42nd	Prod. One	8.6 years	42.4264E+01	328.0
43rd	Prod. One	11.5 years	42.4264E+01	336.0
44th	Prod. One	22.4 years	84.8528E+01	344.0
45th	Prod. One	200.0 years	84.8528E+01	352.0

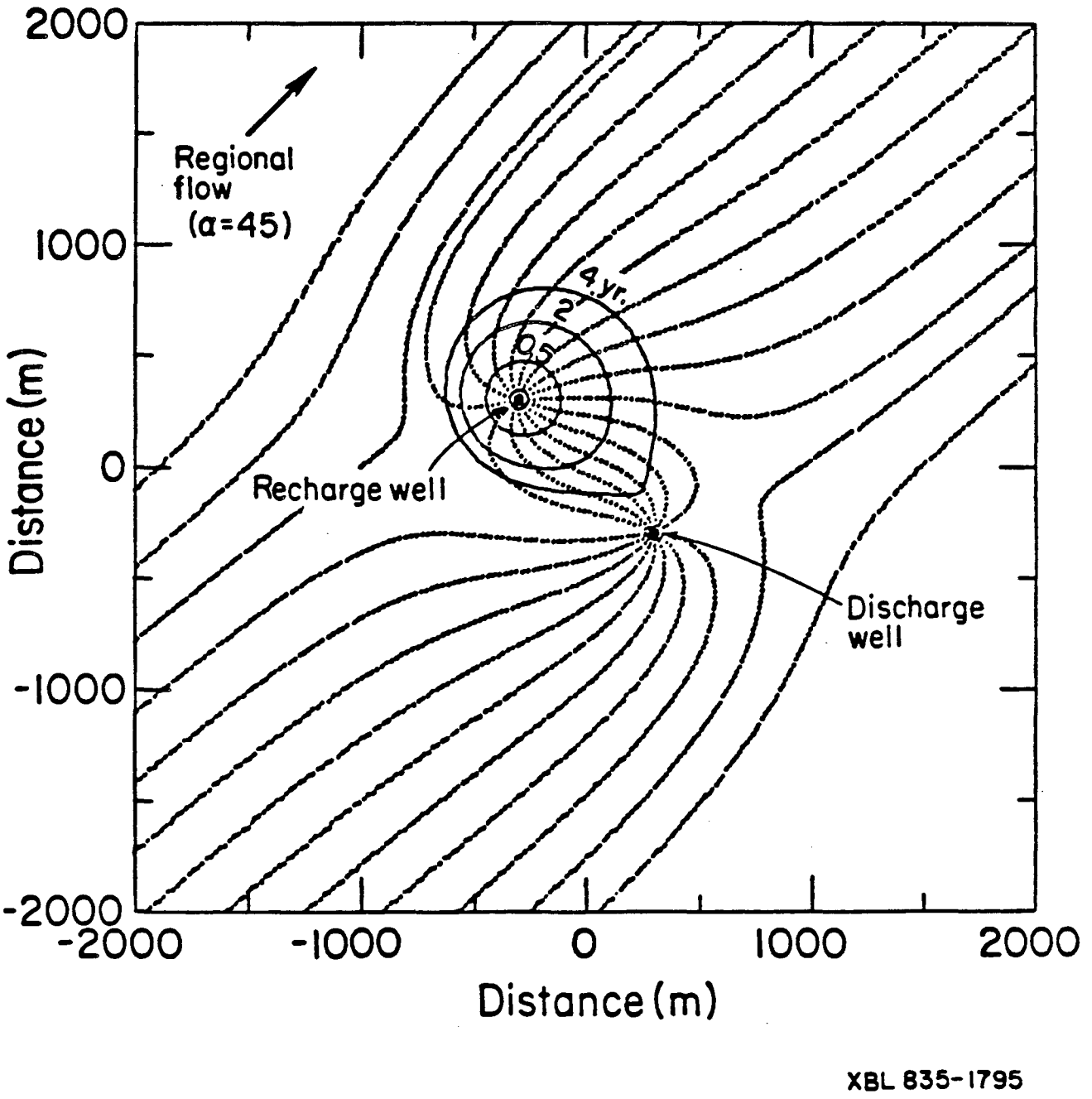

Figure 13. Streamlines and position of injected wastewater front for RESSQ model with regional flow considered.

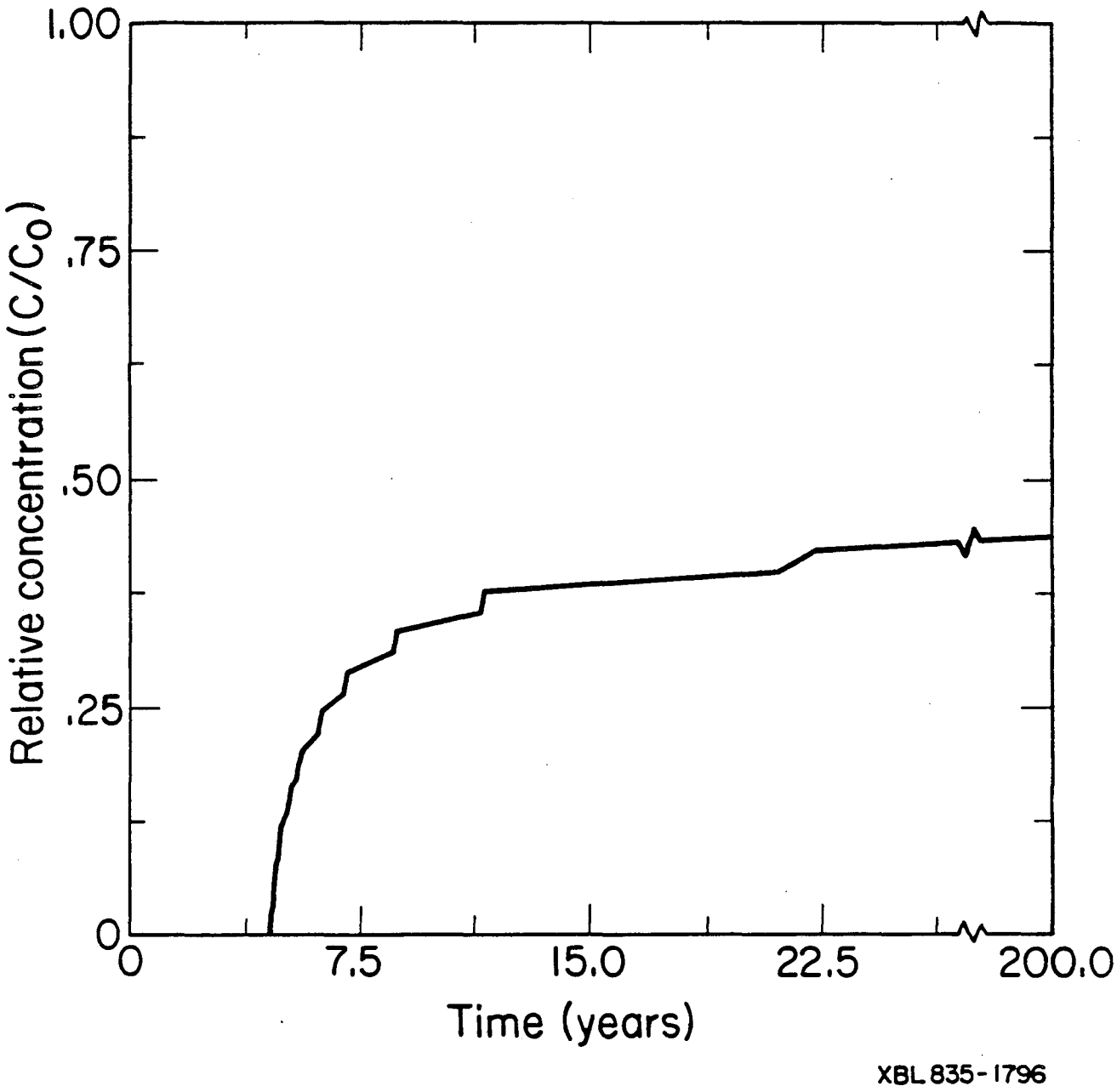

Figure 14. Time variation of relative concentration of water supply well with regional flow considered.

These few examples have been offered to illustrate the power and the simplicity of some analytical techniques, primarily velocity plots, to rapidly estimate the impact to pumping wells from nearby contaminant plumes. As indicated throughout, a wide variety of situations can be examined.

SUMMARY

Data from pumping (water supply) wells are often gathered during ground water contaminant investigations to augment special monitoring wells and to estimate the effectiveness of remedial actions. Because the interpretation of these data requires an understanding of the areal limits of the zone of the aquifer actually yielding waters to a pumping well (the capture zone), it is useful to construct velocity distribution plots. While manual plots are easily constructed for a single well, use of computerized codes is much more efficient for more complex situations. Such codes can be devised to show not only the spatial distribution of contaminants, but also the contaminant concentration history at selected points. Use of such plots can help the field investigator select the most appropriate solutions to pollution problems.

ACKNOWLEDGEMENTS

Continuing cooperation and assistance from I. Javandel and C. Doughty are much appreciated. The work was performed pursuant to Interagency Agreement Number AD 89F 2A 175 between the U. S. Environmental Protection Agency and the U. S. Department of Energy under Contract Number DE-AC03-76SF00098.

REFERENCES

American Petroleum Institute, 1972. The migration of petroleum products in soil and ground water--principles and countermeasures. American Petroleum Institute publication no. 4149, American petroleum Institute, Washington, D. C.

Gibb, J. P., R. M. Schuller, and R. A. Griffin, 1981. Procedures for the collection of representative water quality data from monitoring wells. State of Illinois Department of Energy and Natural Resources Cooperative Ground Water Report No. 7, Illinois State Water Survey, Illinois State Geological Survey, Champaign, Illinois.

Javandel, I., C. Doughty, and C. F. Tsang, 1983a. A handbook for the use of mathematical models for subsurface contaminant transport assessments: Volume 1 - Detailed development and applications. Lawrence Berkeley Laboratory, Berkeley, California.

Javandel, I., C. Doughty, C. F. Tsang, and J. F. Keely, 1983b. A handbook for the use of mathematical models for subsurface contaminant transport assessment: Volume 2 - A simplified guide. U. S. Environmental Protection Agency and Lawrence Berkeley Laboratory.

Keely, J. F., 1982. Chemical time series sampling - a necessary technique. Ground Water Monitoring Review, vol. 2, no. 4.

Keely, J. F. and F. Wolf, 1983. Field applications of chemical time-series sampling. Presented to the Third National Symposium on Aquifer Restoration and Ground Water Monitoring, Columbus, Ohio, May 1983; and submitted to Ground Water Monitoring Review.

Keith, S. J., L. G. Wilson, H. R. Fitch, and D. M. Esposito, 1983. Sources of spatial-temporal variability in ground water quality data and methods of control. Ground Water Monitoring Review, vol. 3, no. 2.

Nacht, S. J., 1983. Groundwater monitoring system considerations. Ground Water Monitoring Review, vol. 3, no. 2.

Schuller, R. M., J. P. Gibb, and R. A. Griffin, 1981. Recommended sampling procedures for monitoring wells. Ground Water Monitoring Review, vol. 1, no. 1.

Schmidt, K. D., 1977. Water quality variations for pumping wells. Ground Water, vol. 15, no. 2.

Schmidt, K. D., 1982. How representative are water samples collected from wells? Proceedings of the Second National Symposium on Aquifer Restoration and Ground Water Monitoring, Natural Water Well Association, Columbus, Ohio.

Todd, D. K., 1980. Groundwater Hydrology, 2nd edition, John Wiley and Sons, New York, N. Y.

Warner, D. L., and M. G. Yow, 1979. Programmable hand calculator program for pumping and injection wells: I - Constant or variable pumping (injection) rate, single or multiple fully penetrating wells. Ground Water, vol. 17, no. 6.

LIST OF FIGURES

This report was done with support from the Department of Energy. Any conclusions or opinions expressed in this report represent solely those of the author(s) and not necessarily those of The Regents of the University of California, the Lawrence Berkeley Laboratory or the Department of Energy.

Reference to a company or product name does not imply approval or recommendation of the product by the University of California or the U.S. Department of Energy to the exclusion of others that may be suitable.

TECHNICAL INFORMATION DEPARTMENT
LAWRENCE BERKELEY LABORATORY
UNIVERSITY OF CALIFORNIA
BERKELEY, CALIFORNIA 94720